H13-49
UPWARD AND SIDEWARD REMOVAL OF AIR POLLUTANTS IN THREE-DIMENSIONAL STREET CANYONS

Pei Shui, Chun-Ho Liu and Yuguo Li

Department of Mechanical Engineering, The University of Hong Kong, Pokfulam Road, Hong Kong, China

Abstract: The problems of ventilation and pollutant removal in urban areas have been mainly studied based on the idealized two-dimensional (2D) street canyons. These researches have enriched our understanding of pollutant transport in infinitely long streets but have often overlooked the processes via the ends of the streets. In this paper, we focused on the ventilation and pollutant transport in idealized three-dimensional (3D) street canyons instead. Computational fluid dynamic (CFD) models with unsteady Reynolds-averaged Navier-Stokes (URANS) Renormalization group (RNG) k-ε turbulence model were adopted. The homogeneous building geometry at the bottom was constructed by an array of identical cubes. An area source of uniform pollutant concentration was applied on the ground in one of the street canyons. A series of sensitivity tests were performed to examine the effects of building-breadth-to-street-width ratio (WR) on the pollutant transport behaviours. It was found that the pollutant is transported as a plume in the shear layer and in the form of channelling below the canopy level. Both the ventilation and pollutant removal exhibit oscillating behaviours, thus averaging in the temporal domain was carried out to determine the mean effects. The pollutant removal is divided into two components, by turbulence or by mean flow, to elucidate the mechanism. The finding shows the contribution to pollutant re-entrainment from the roof level or the street ends. When the street length in the y direction is wider, the ventilation and pollutant removal show obvious oscillations in which both the mean and the turbulent components remove a significant amount of pollutant through the ends to the streets. These results imply that the influence of sideward pollutant transport to pollutant transport in the streamwise direction in street canyons of different WR is significant. The results based on idealized 2D street canyons should be interpreted with caution for more accurate analysis.

Key words: 3D model, street canyon, pollutant transport, air ventilation

1 INTRODUCTION

2D street canyons are designed for our fundamental understanding of ventilation and pollutant removal in idealized units but it is rarely used in practice. The 2D geometric assumption results in upward pollutant removal through the street roof only. The sideward pollutant removal from the street canyon through the street ends is overlooked that apparently suppresses the ventilation and pollutant removal. The oscillating properties in the 3D simulation (Kanda, Moriwaki et al. 2004) also challenge the pseudo-state assumption in 2-D model. Raupach and Coppin et al. (1986) performed a wind tunnel experiment with tall thin strips as the 3-D city models and concentrated on the influence of frontal area index (density). Their measurements showed the dominance of large eddies in the boundary layer that moves downstream with a height-independent prevalent flow. Macdonald and Griffiths et al. (1998) investigated the transport of pollutant being emitted from a point source in and over an array of cubes (square and staggered array were measured). Both wind tunnel experiments and field measurements demonstrated the significantly different patterns between the 3-D and 2-D models. Afterwards, they refined the empirical constant C_μ in the k-ε model and suggested a series of scaling ratios for turbulence variances in different dimensions (Macdonald, Carter Schofield et al. 2002). The findings in that research were also in line with others (Cermak 1995, Grimmond and Oke 1999) that formulated the vertical wind profile as a function of plan area density and frontal area density. Cheng and Castro (2002) also designed another wind tunnel experiment with staggered array and confirmed the strong 3D turbulent flow in the roughness sublayer. Yee and Gailis et al. (2006) compared their results among wind tunnel, water channel and field measurements. The good agreement suggested that when the Reynolds number was large enough to maintain fully turbulent flows within the obstacle array, their effects on pollutant mixing rates are small. Apart from these experiments, Lien and Yee (2004) simulated the turbulence development in a 3D building array using the RANS k-ε model. The results were used to diagnose the dispersive stress, within and above the building array. Kanda (2006) investigated the turbulence organized structures above square and staggered building arrays with LES model. Based on their results, it was suggested that the geometry property of a canopy must be considered as an important parameter when analyzing pollutant dispersion efficiency. This research will take Macdonald's field measurement as the validation, and compare the sideward/upward pollutant transport of the canyon with the pollutant source and its downwind neighbouring canyons under different geometry settings, including their individual contributions to both pollutant removal and re-entrainment.

2 Methodology
2.1 Computational Domain and Boundary Conditions

Figure 1 is the current 3D computational domain. Free stream travels through the domain in the *x* direction. The building breadth in streamwise direction (*a*), the building height (*h*, not shown in the figure) and distance between buildings (*d* in *y* direction and *b* in *x* direction) are all kept constant. Only the building breadth in *y* direction (*w*) is changed to control the street canyon building-breadth-to-street-width ratio *w/b*. The computational domain comprises of 40 identical street canyons (8 are aligned in the streamwise direction and 5 in the spanwise direction) under the shear layer. The boundary condition in the inlet is the power law adopted by Macdonald's wind tunnel experiments (streamwise velocity profile $U(z) = 0.15(z_f/h_f)^{0.26}$. The symmetry boundary condition is assumed at the top of the shear
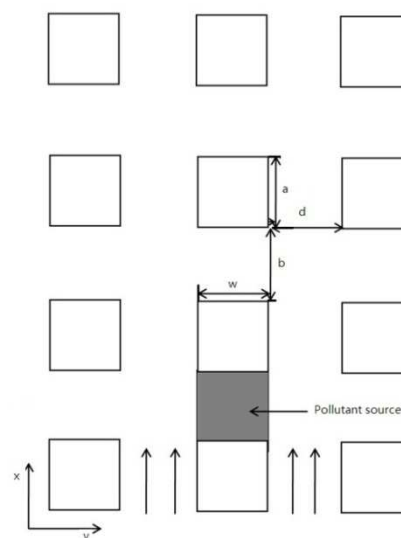

Figure 7 Computational domain (plane view)

layer and the side of the domain. All the facades, roofs and grounds are set as non-slip wall and with standard wall function. In this study, the dimensionless wall distance y+ was controlled beyond a minimum of 11 to assure the adaptability of the wall treatments. An area source with uniform dimensionless constant pollutant concentration 1 is prescribed on the ground of the central street canyon (A) for our sensitivity analysis, while a point source with constant pollutant emission rate is set in front of the obstacle in the validation case. Re $(=U_0 h/\nu)$ is equal to 15,000 approximately which is high enough for the flow independence from viscosity (Pavageau and Schatzmann 1999). The simulations were carried out by OpenFOAM using rectangular mesh. The canyon allocated with the pollutant source and its neighbouring canyons were vested with finer meshes compare to other regions to study. The dense-mesh regions have 30 grids per unit length, and the results are comparable to those of the coarse mesh, suggesting the grid-independent calculations.

2.2 Mathematical Equations

The RANS model was used in this paper to simulate the flow in which all the variables have two components: mean component (described by " $\overline{}$ ") and fluctuating component (described by " ' "). The Renormalization Group (RNG) k-ε turbulence model (Yakhot and Orszag 1986) was implemented with two additional transport equations for turbulence kinetic energy (k) and dissipation (ε), and modified the epsilon equation by changing the production term to account for the different scales of motion. A transport equation for passive scalar representing the pollutant transport was added in the RANS form:

$$\frac{\partial \bar{c}}{\partial t} + \frac{\partial}{\partial x_i}\left(\overline{u_i}\bar{c} - D_t \frac{\partial}{\partial x_i}\bar{c}\right) = S \tag{1}$$

Here, D_t $(= \nu_t/\text{Sc}$, where $\text{Sc} = 0.72$ is the Schmidt number) is the turbulent pollutant diffusivity and $\bar{c}$ is the pollutant concentration. The first and second terms inside the bracket of Equation (1) represent the convection and diffusion of pollutant, respectively.

The ventilation rate (ACH) was decomposed to mean component and fluctuating component and so did the pollutant removal rate (PCH). This approach allowed us to examine the contribution of each component under different cases.

$$\text{ACH} = \overline{\text{ACH}} + \text{ACH'} = \int_\Gamma \overline{u_{n_+}}\,dA + \int_\Gamma \sqrt{u_n'u_n'}\,dA = \int_\Gamma \overline{u_{n_+}}\,dA + \int_\Gamma \sqrt{-\frac{1}{2}\nu_t\frac{\partial \overline{u_n}}{\partial n} + \frac{1}{6}k}\,dA \tag{2}$$

$$\text{PCH} = \overline{\text{PCH}} + \text{PCH'} = \int_\Gamma \overline{u_n}\bar{c}\,dA + \int_\Gamma u_{n_t}c_t\,dA = \int_\Gamma \overline{u_n}\bar{c}\,dA - \int_\Gamma D_t\frac{\partial \bar{c}}{\partial n}\,dA \tag{3}$$

Where the ACH' was deduced from Reynolds stress tensor:

$$R_{ij} = -\overline{u_i'u_j'} = \nu_t\left(\frac{\partial \overline{u_i}}{\partial x_j} + \frac{\partial \overline{u_j}}{\partial x_i}\right) - \frac{2}{3}\delta_{ij}k \tag{4}$$

Different street widths will provide the pollutant source in different scale. Apart from ACH and PCH, the spatial average pollutant concentration is another important parameter that directly measures the air pollutant level:

$$\langle C \rangle = \int_V \bar{c}\,dV/V \tag{5}$$

Because of the strong oscillating behaviours exhibited by the 3-D model during the simulation, a time average approach was adopted to analyse all the variables.

$$\tilde{\phi} = \int_T \bar{\phi}\,dt/T \tag{6}$$

The over bar of $\bar{\phi}$ means the time average of a very short instance refer to the fluctuating caused by the turbulence, while $\tilde{\phi}$ means the average in the sampling time.

3 Model Validations

The wind tunnel experiment and filed measurement concentrated on scalar dispersion (Macdonald, 1998) and flow field (Macdonald, 2002) of the 3-D cube array were employed in the validation exercise of this study. The difference between the simulation and experiment was controlled as small as possible. The profiles of velocity, k and normalized pollutant concentration are compared in Figures 2. The pollutant concentration is normalized by:

$$C_K = CUH^2/Q \tag{7}$$

Here C is the pollutant concentration, U is the reference velocity, H is the obstacle reference height and Q is the pollutant source emitting rate.
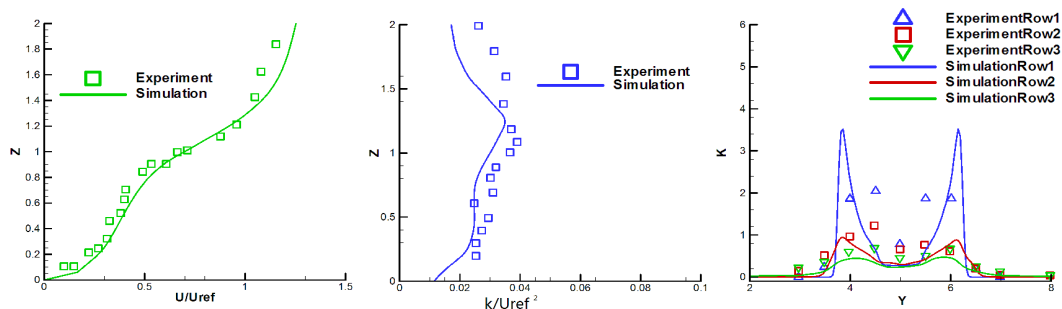

Figure 8 Comparison between experiment and simulation. (a) velocity profile; (b) turbulence kinetic energy profile sampled at the 7th row behind the street; (c) C_K profil, sampled at 1st, 2nd, 3rd row behind the street.

4 Results and Discussions
4.1 WR1

Figure 3 reports the oscillation of the spatial averaged pollutant concentration inside the street canyon of WR = 1. The sample was started to collect at 3000s, after the prevalent flow had already travelled the whole computational domain over 20 times, and lasted for 600s, which consists of 3 circles. In such case, w=1, the buildings are standard cubes. The ACH has little difference between each canyon (<5% in Table 1), the results show that the ventilation calculation would not be affected by the boundary and the size of the computational domain, and provide a suitable surrounding to study the pollutant transport. Both along the upward and sideward interface, is the major process especially in the upward direction.
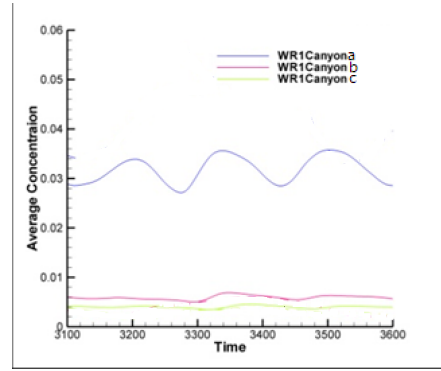
For the canyon A (the one with the pollutant source), both the upward and sideward interface have their contribution to pollutant removal. However, the component which contributes more in these two directions is different. As shown in Table 1, at the upward interface, the turbulence component

Figure 9 Averaged pollutant concentration versus time for WR1

( ) dominates the pollutant removal, and the mean flow could only carry a very small amount of pollutant back into the street canyon. In the sideward direction, the pollutant removed by turbulence is in the same scale as the upward interface, however as this interface is directly linked to the ground pollutant source, the pollutant removed by the mean flow becomes the majority, which have a significant larger level. For the downwind neighbouring street canyons (B), we can learn that the pollutant is entering the canyon from the side and leaving from the top.

Table1 PCH and ACH preference in each interface of WR1

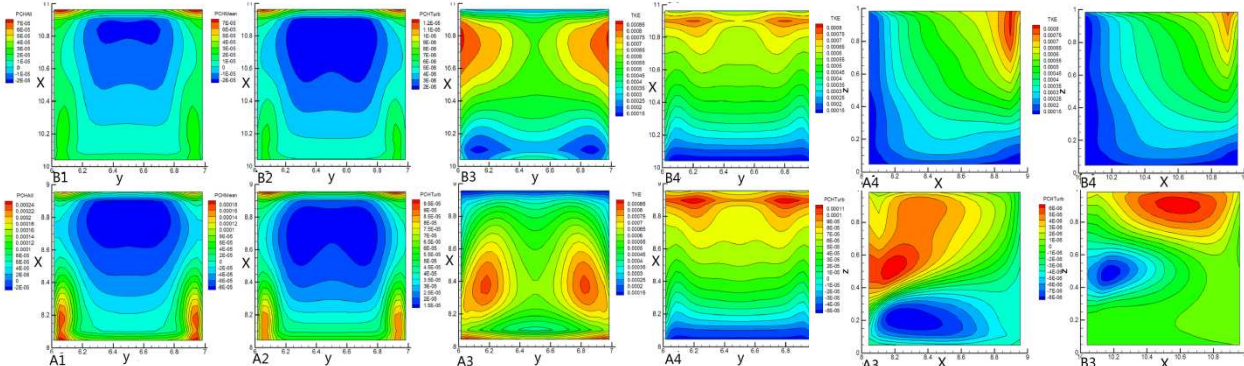| Canyon-interface	PCH(m/s)	(m/s)	(m/s)	ACH(m/s)	(m/s)	(m/s)
a-Upward	6.01E-05	-4.65E-06	6.48E-05	1.22E-02	2.68E-03	9.52E-03
b-Upward	5.22E-06	-2.38E-06	7.60E-06	1.15E-02	2.40E-03	9.10E-03
a-Sideward	2.74E-04	2.37E-04	3.69E-05	1.30E-02	5.19E-03	7.81E-03
b-Sideward	-3.08E-06	-3.00E-06	-8.92E-08	1.23E-02	4.94E-03	7.36E-03

Figure 10 Upward interface contours of WR1, A and B refers to canyons and 1: PCH; 2: ; 3: ; 4: Turbulence kinetic energy.

Figures 4 and 5 depict the PCH distribution in the upward and sideward interface. From the figures, we can find the PCH contours are very close to , which implies that in most individual position, dominates the local pollutant transport. However, those transport processes perform not only removal but also entrainment. At the canyon top, these two contrast effects finally present the as a subordinate component for pollutant removal (Figure 4-A,B-1, 4-A,B-2). For the sideward direction, a strong spanwise (axis in *x* direction) rotation inside the street canyon carries the pollutant out of the canyon at the ground level and take in at the upper level. As the mean flow near the ground could carry a large amount of pollutant directly from the source canyon, the overall perform a very large positive value compared with its upward counterpart in canyon A. In the neighbouring canyons, as the ventilation effect is still significant, and the pollutant from source will move

Figure 11 Sideward interface contours

upward by both ventilation and diffusion, the pollutant entrainment led by the spanwise rotation in upper of sideward interface is significant, while the ground without source has much less pollutant to travel out, the overall performs a large negative value (Figure 5-A,B-2).

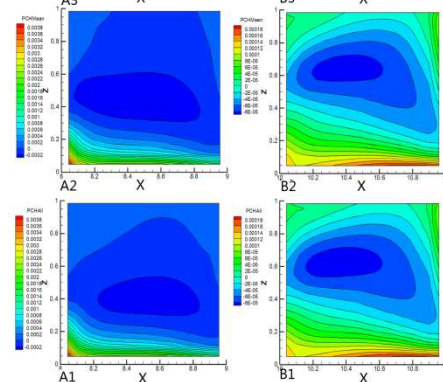Figures 4 & 5 also suggest that the peaks of   (which is the major contribution to the fluctuating component of pollutant removal) of upward and sideward are actually belong to one region in each canyon (Figure 4-A,B-3, Figure 5-A,B-3). However, this high   are in the different position of the two canyons. In Figure 4-B-3, we can find in the neighbouring canyon, the peaks of the   are close to the peak of the k (Figure 4-B-4), and in the source canyon, the peaks of   (Figure 4-A-3) is allocated in the contrast direction of the k (Figure 4-A-4). Equation (3) indicates the   depends on both the pollutant concentration and turbulence. When pollutant emits from the source canyon, as the concentration is higher, especially in the leeward facade where the pollutant is accumulated by the main circulation, the distribution of pollutant decides the   in the top of the canyon A, while in canyon B which have less pollutant scale, the turbulence scale control the   .

4.2 WR2
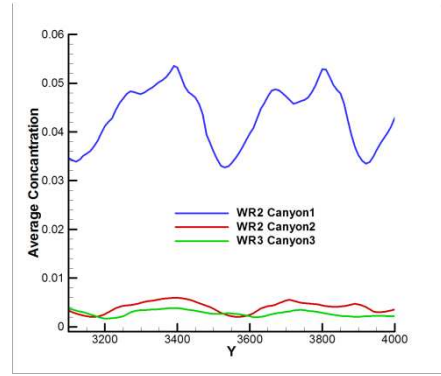

Figure 12 Averaged pollutant concentration versus time for WR2
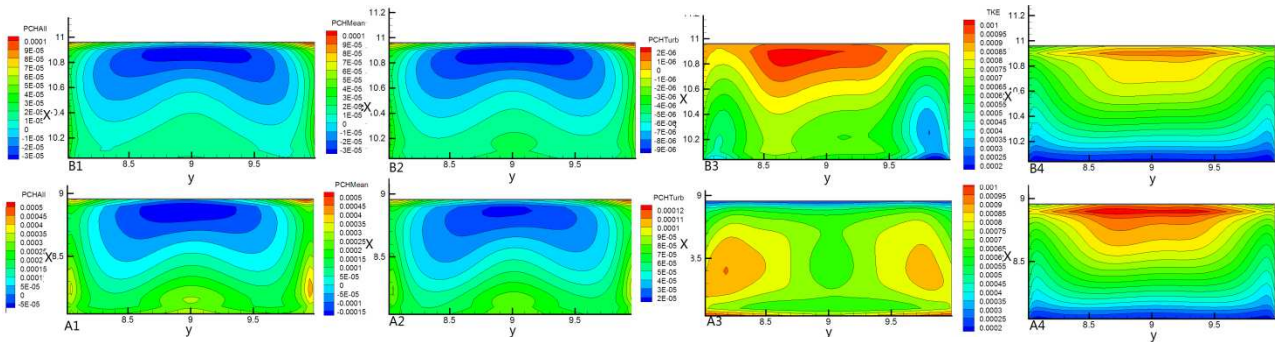

Figure 13 Upward interface contours of WR2

Figure 6 depicts the average concentration of the canyon A and B when the building width is 2m. The period of the curve increases from near 200s in previous case to about 400s, while the amplitude increases also in the same scale. Furthermore, different from the previous case that   was always larger than   , here the difference between them becomes less and some time   is even smaller than   , which implies an interesting conclusion: in certain case, far away from the pollutant source may not lead to a better air quality. Table 2 lists the difference compared with the previous case: Though the upward interface area of the street canyon is increased about 2 times, the ACH increase little. The comparison between Tables 1 and 2 shows that   is actually increased (by about 1.5 times) while   has nearly no improvement. Since   is the major portion of the total ACH, this results in the poor amelioration of air ventilation.

However, the changing of ACH structure has much more influence to the PCH composing than to itself. In the upward interface of source canyon,   and TKE follow the similar pattern of previous case and simply increases in the same level as   while   increases greatly. Compare Figure 4-A-2 and Figure 7-A-2, in both settings, the negative   is allocated near the windward face end, and the positive   is concentrated at the leeward face central. This PCH distribution is the result of the air ventilation. As the air in the artery is directly driven by the free stream and has a higher velocity, the flow inside the street canyon is blocked inside and forms the sub-recirculation (axis in z). This cause of formation is similar to the main-recirculation (axis in y) inside the canyon driven by the free stream, but weaker because the channelling flows in the artery are weaker than the free stream. As a result, the pollutant would be accumulated in the leeward central facade, and removed by main-recirculation. (Figure 9)The wider street allows the full development of this sub recirculation and therefore improves   . As for the sideward interface, the two cases follow the similar pattern, and the each components of PCH just simply increases by about 1.5 times.
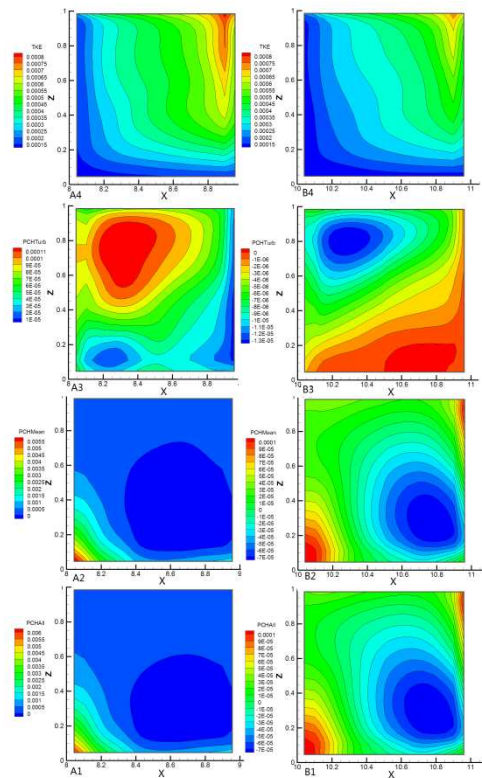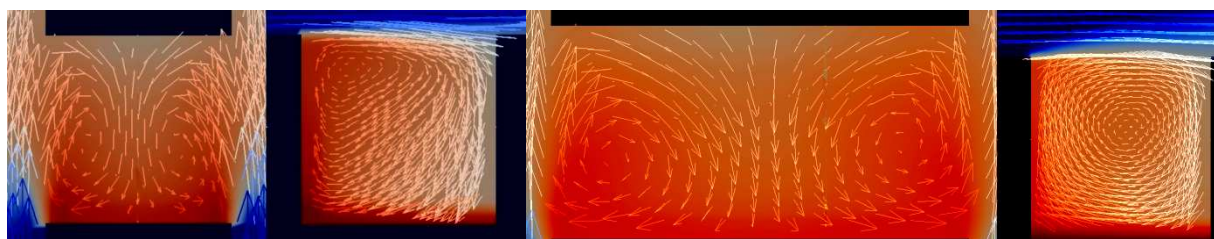

Figure 14 Sideward interface contours PF wr2:

a-1 upward vision for WR=1 a-2 sideward vision for WR=1 b-1 upward vision for WR=2   b-2 sideward vision for WR=2

Figure 15 Velocity vector counters, background colour represents the pollutant concentration

The change of pollutant removal pattern in canyon A affects the canyon B deeply. Compare the quotient of sideward PCH over upward PCH in WR1 (4.56) and WR2 (2.71), the pollutant prefer transfer to canopy when street is wider, which means less possible to enter other canyons by ground channelling flow. Figure 4 and Figure 6 show that the   in canyon B of WR2 is smaller than that of WR1, and this lower   results in negative   (pollutant entrainment) in both upward and sideward interface. Compare Table1 and Tabel2, the upper part has positive   in WR1 while negative in WR2 for canyon B, just implies the   there is relatively lower in WR1 and higher in WR2.

Table2 PCH and ACH preference in each interface of WR2

Canyon-interface	PCH(m/s)	(m/s)	(m/s)	ACH(m/s)	(m/s)	(m/s)
A-Upward	1.54E-04	6.40E-05	9.02E-05	1.39E-02	3.76E-03	1.02E-02
B-Upward	4.24E-06	6.93E-06	-2.69E-06	1.33E-02	3.49E-03	9.80E-03
A-Sideward	4.18E-04	3.53E-04	6.47E-05	1.58E-02	7.90E-03	7.86E-03
B-Sideward	-2.60E-06	3.37E-06	-5.97E-06	1.43E-02	7.36E-03	6.95E-03

5 Conclusions

From the results and analysis, we can draw the following conclusions: First, the pollutant transport has strong oscillating behaviours in the 3D-street canyon, and the extension of the street width would increase the oscillating circle period; second, in most part of interface, the mean flow dominates the local pollutant transfer, however, the turbulence bring more pollutant through the upwards interface out of the source canyon. For the sideward interfaces, as the recirculation can blow the pollutant directly from the ground source, the mean component dominates the pollutant removal from the source canyon. Generally speaking, the pollutant enters from the sideward interface and emit from the upward in the neighbouring canyon. The difference is, the wider canyon allows larger pollutant capacity inside the canyon, which maintains a relatively smaller pollutant concentration inside and this difference leads to the neighbouring canyon a positive upward   when WR=1 but negative when WR=2.

REFERENCES

Cermak, J. E., Ed. (1995). Wind Climate in Cities, Kluwer Academic Publishers. Printed in the Netherlands.

Cheng, H. and I. P. Castro (2002). "Near Wall Flow over Urban-like Roughness." Boundary-Layer Meteorology **104**(2): 229-259.

Grimmond, C. S. B. and T. R. Oke (1999). "Aerodynamic Properties of Urban Areas Derived from Analysis of Surface Form." Journal of Applied Meteorology **38**(9): 1262-1292.

Kanda, M. (2006). "Large-Eddy Simulations on the Effects of Surface Geometry of Building Arrays on Turbulent Organized Structures." Boundary-Layer Meteorology **118**(1): 151-168.

Kanda, M., R. Moriwaki, et al. (2004). "Large-Eddy Simulation of Turbulent Organized Structures within and above Explicitly Resolved Cube Arrays." Boundary-Layer Meteorology **112**(2): 343-368.

Lien, F.-S. and E. Yee (2004). "Numerical Modelling of the Turbulent Flow Developing Within and Over a 3-D Building Array, Part I: A High-Resolution Reynolds-Averaged Navier—Stokes Approach." Boundary-Layer Meteorology **112**(3): 427-466.

Macdonald, R. W., S. Carter Schofield, et al. (2002). "Physical Modelling of Urban Roughness using Arrays of Regular Roughness Elements." Water, Air, & Soil Pollution: Focus **2**(5): 541-554.

Macdonald, R. W., R. F. Griffiths, et al. (1998). "A comparison of results from scaled field and wind tunnel modelling of dispersion in arrays of obstacles." Atmospheric Environment **32**(22): 3845-3862.

Pavageau, M. and M. Schatzmann (1999). "Wind tunnel measurements of concentration fluctuations in an urban street canyon." Atmospheric Environment **33**(24-25): 3961-3971.

Raupach, M. R., P. A. Coppin, et al. (1986). "Experiments on scalar dispersion within a model plant canopy part I: The turbulence structure." Boundary-Layer Meteorology **35**(1): 21-52.

Yakhot, V. and S. A. Orszag (1986). "Renormalization group analysis of turbulence. I. Basic theory." Journal of Scientific Computing **1**(1): 3-51.

Yee, E., R. Gailis, et al. (2006). "Comparison of Wind-tunnel and Water-channel Simulations of Plume Dispersion through a Large Array of Obstacles with a Scaled Field Experiment." Boundary-Layer Meteorology **121**(3): 389-432.